The possible changes both of $k^{18}O$ and s would therefore lead to higher d values at glacial periods. Anyway, the influence of variations of $k^{18}O$ and s for the first part of the water cycle is small. The effect of a more hypothetical slope change at snow formation was not estimated but if it exists the present interpretation of higher relative humidity would be also reinforced. This last point could be investigated from the comparison with d data obtained on other, existing or future, ice cores. (Note, however, that interpretation of data from more coastal Antarctic sites will be complicated by the change in snow origin.) More generally, it would be very interesting to compare the Dome C d profile with that in other ice cores both from Greenland and Antarctic ice sheets.

From energy balance considerations, ~10% less evaporation would be anticipated[30]. Atmospheric modelling of ice age climate shows a comparable decrease[27]. Taking into account the 2 °C reduction of the sea-surface temperature[11], leading to an average reduction of q_s of ~15%, equation (5) shows that a 10% decrease of evaporation, as suggested above, is obtained by keeping the $(1-h)U$ value practically unchanged. An h value of 90% (instead of 80%), as suggested by d changes, thus infers, on average, a doubling of the wind speed over all the oceanic area concerned. Although these are many assumptions in such an interpretation, it does point out the high consistency of two experimental results from the Dome C ice core at 18,000 yr BP, that is, a lower d value and high Na (and also aerosols) content, indicating respectively a higher relative humidity close to the oceanic surface and a higher wind speed.

Remarkably, such a correlation between d and Na profiles exists all along the core (Fig. 1), tending to show that relative humidity and wind speed vary in a parallel manner with values for stages 2 and 4 in between those prevailing during the Holocene and maximum glacial periods. The entire d profile clearly contains interesting information regarding the relative humidity changes over the past 32,000 yr. For example, relatively low d values encountered around 4,000 yr BP (Fig. 1*b*) coincide with the drier climates that have characterized the past 4,000–4,500 yr (ref. 31). This is in agreement with the fact that a d decrease probably reflects an h increase which means (neglecting the possible changes of U and q_s), a reduction of the evaporation rate (equation (5)). It is also observed that the wet phase ending 25,000 yr BP in southern Australia presents higher d values than the following drier 25,000–14,000 yr BP period[32]. Dating uncertainties prevent detailed discussion of the synchronism between d and wetness changes but changes from wet to dry conditions are apparently accompanied by a d decrease and vice versa, which is quite consistent with our interpretation on d changes.

However, at its present stage of interpretation, the main result of this study is the strong indication of higher relative humidity over the ocean surface (estimated around 90%) south of 40° S during the late glacial maximum. A similar change probably also affected the tropical and equatorial regions as suggested either from isotopic data[6,7] or from theoretical considerations[33]. Such data have probably to be taken into account when developing climate modelling of the ice age.

This work was supported by Terres Australes et Antarctiques Françaises, NSF (Division of Polar Programs), DGRST and INAG. We thank all those who helped in drilling the core, M. Pourchet for sampling of the ice core increments, R. Chiron for isotopic measurements, J. R. Petit for helpful discussions, J. P. Benoist for data processing and M. Briat for the Na data.

Received 12 May; accepted 9 August 1982.

1. Craig, H. *Science* **133,** 1702–1793 (1961).
2. Dansgaard, W. *Tellus* **16,** 436–468 (1964).
3. Gat, J. R. *Handbook of Environmental Isotope Chemistry* Vol. 1 (eds Fritz, P. & Fontes, J. C.) 21–48 (Elsevier, Amsterdam, 1980).
4. Dansgaard, W., Johnsen, S. J., Moller, J. & Langway C. C. *Science* **166,** 377–381 (1969).
5. Epstein, S., Sharp, R. P. & Gow, A. J. *Science* **168,** 1570–1572 (1970).
6. Sonntag, C. *et al. Isotope Hydrology*, 569–581 (IAEA, Vienna, 1978).
7. Merlivat, L. & Jouzel, J. *J. geophys. Res.* **84,** 5029–5033 (1979).
8. Harmon, R. S. & Schwarcz, H. P. *Nature* **290,** 125–128 (1981).
9. Lorius, C., Merlivat, L., Jouzel, J. & Pourchet, M. *Nature* **280,** 5724, 644–648 (1979).
10. Hays, J. D., Imbrie, J. & Shackleton, N. J. *Science* **194,** 1121–1132 (1976).
11. Climap Project Members *Science* **191,** 1131–1137 (1976).
12. Hageman, R. & Lohez, P. *Adv. Mass spectrometry* **7,** 504–507 (1978).
13. Johnson, S. J. *IAHS Publ.* No. 118, 210–219 (1977).
14. Dansgaard, W. & Tauber, H. *Science* **166,** 499–502 (1969).
15. Moser, H. & Stichler, W. *IASH Publ.* **114,** 122–135 (1975).
16. Jouzel, J., Merlivat, L., Petit, J. R. & Lorius, C. *J. geophys. Res.* (submitted).
17. Merlivat, L. *J. geophys. Res.* **83,** 2977–2980 (1978).
18. Ericsson, E. & Bolin, B. *Proc. 2nd Conf. on Radioactive Fallout from Nuclear Weapon Tests* (AEC) 675–686 (1964).
19. Manabe, S., Smagorinski, J. & Strickler, R. *Mon. Weath. Rev.* **93,** 769–798 (1965).
20. Kangos, J. D. *J. geophys. Res.* **65,** 4007–4012 (1960).
21. Friedman, I., Redfield, A. C., Schoen, B. & Harris, J. *Rev. Geophys.* **2,** 1, 177–224 (1964).
22. Newton, C. W. *Met. Mon.* **13,** 215–246 (1972).
23. Taljaard, J. J. *Met. Mon.* **13,** 139–214 (1972).
24. Van Loon, H. *Met. Mon.* **13,** 87–100 (1972).
25. Petit, J. R., Briat, M. & Royer, A. *Nature* **293,** 391–394 (1981).
26. Manabe, S. & Hahn, D. G. *J. geophys. Res.* **82,** 3889–3911 (1977).
27. Gates, W. L. *J. atomos. Sci.* **33,** 1844–1873 (1976).
28. Morelli, J. thesis, Univ. Paris (1968).
29. Podzimek, J. *J. Rech. Atmos.* **14,** 35–61 (1980).
30. Newell, R. E. & Herman, G. F. *WMO/IAMAP* **421,** 293–300 (1975).
31. Talbot, M. R. *Quat. Res.* **16,** 201–220 (1981).
32. Bowler, J. M. in *Antarctic Glacial History and World Paleoenvironments* (ed. Van Zinderen Bakker, E. M.) 149–172 (Balkema, Rotterdam, 1978).
33. Flohn, H. in *Climatic Variations and Variability: Facts and Theories* Vol. 72 (Serie C) 233–232 (NATO, 1981).

Signal recognition particle contains a 7S RNA essential for protein translocation across the endoplasmic reticulum

Peter Walter & Günter Blobel

The Rockefeller University, New York, New York 10021, USA

In addition to its previously characterized, six different polypeptide components, signal recognition protein—which functions in protein translocation across and integration into the endoplasmic reticulum membrane—contains a 7S RNA molecule. The RNA is closely identified with the small cytoplasmic 7SL RNA and is required for both structural and functional properties of signal recognition protein—which we therefore rename signal recognition particle.

THE signal recognition protein (SRP) has been previously isolated as an 11S complex consisting of six distinct polypeptide chains[1] from a salt-wash of microsomal vesicles[2], and is an essential component in the process of protein translocation across the lipid bilayer of the endoplasmic reticulum[1]. SRP functions in decoding the information contained in the signal peptide of nascent secretory[3–5], lysosomal (A.H. Erickson, P.W. and G.B., in preparation) and certain membrane[6] proteins to

0028–0836/82/420691—02$01.00

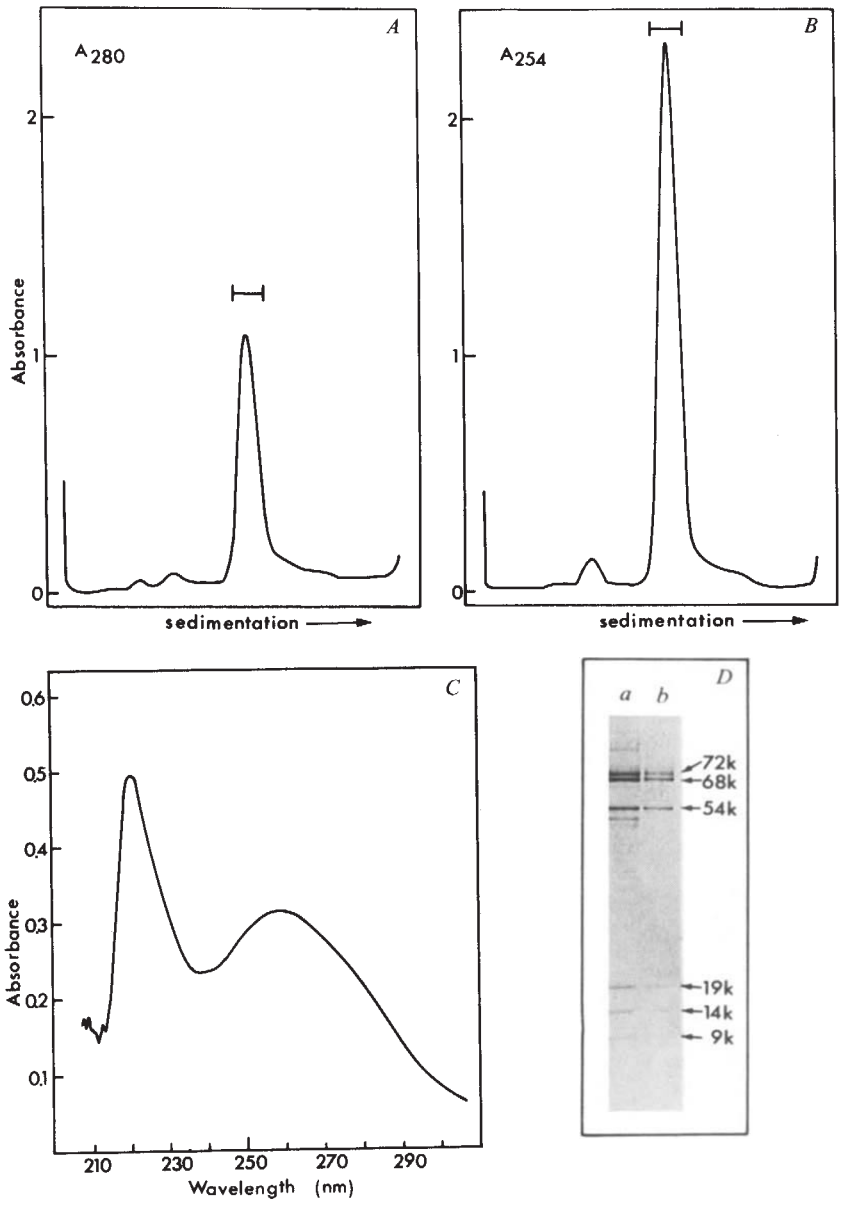

Fig. 1 Co-purification of SRP and SRP-RNA. SRP was extracted from 500 ml of dog pancreatic microsomes (50 A_{280} units ml^{-1})[3] and purified by chromatography on aminopentyl agarose as described previously[1]. The eluent of the hydrophobic column was diluted with four volumes of water to reduce the salt concentration to 200 mM KOAc and passed over a 10-ml column of DEAE-Sepharose 6B-Cl. The column was washed with 50 ml of a solution containing 50 mM triethanolamine/HOAc *p*H 7.5 (TEA), 350 mM KOAc, 3.5 mM $Mg(OAc)_2$, 1 mM dithiothreitol (DTT), 0.01% Nikkol (nonionic detergent from Nikko)[1] and eluted with a step of a solution containing 50 mM TEA, 600 mM KOAc, 6 mM $Mg(OAc)_2$, 1 mM DTT, 0.01% Nikkol. SRP eluted as a sharp peak (absorbance at 280 nm was monitored) and was collected as a 5-ml fraction (3 A_{280} units ml^{-1}). Aliquots (0.5 ml) of this concentrated SRP solution were layered on top of 5–20% sucrose gradients (12 ml) containing 50 mM TEA, 500 mM KOAc, 5 mM $Mg(OAc)_2$, 1 mM DTT, 0.01% Nikkol and centrifuged for 20 h at 40,000 r.p.m. in the Beckman SW40 rotor as described previously[1]. The gradients were fractionated using an ISCO gradient fractionator with a continuous flow cell (5 mm path length) and the absorbance was recorded at 280 nm (panel *A*) and 254 nm (panel *B*). Sedimentation was from left to right. The 11S peak fraction was collected as indicated by the vertical bar and used for all following experiments. It had a concentration of 1.1 A_{280} units ml^{-1} or 1.6 A_{260} units ml^{-1} and its activity was 20 U μl^{-1} (ref. 1). A 100-μl aliquot of the gradient purified SRP was diluted with 400 μl of water and an absorption spectrum was recorded using a Beckman DU-8 spectrophotometer with wavelength scanning accessory (panel *C*). A 30-μl fraction of the SRP preparation before (panel *D*, lane *a*) and after (panel *D*, lane *b*) sucrose gradient centrifugation was precipitated with trichloroacetic acid (TCA) and subjected to SDS-polyacrylamide gel electrophoresis on 10–15% gradient gels. Polypeptides were visualized by staining with Coomassie blue. The six SRP proteins[1] are indicated with their corresponding molecular weights.

the effect that it mediates the specific attachment of this class of polysomes to the microsomal membrane[7]. In the absence of microsomal membranes SRP specifically arrests the elongation of these proteins *in vitro*[3] just after the signal peptide has emerged from the ribosome, thereby preventing the completion of pre-secretory proteins in the cytoplasm[8]. On interaction of these arrested ribosomes with a specific integral membrane protein—the SRP receptor[9,10]—on the microsomal membrane, this elongation arrest is released and the nascent chain is translocated across[8] or—as in the case of certain integral membrane proteins—integrated into[6] the lipid bilayer.

Several small RNAs have been found and characterized in eukaryotic cells (for a recent review see ref. 11), but besides the tRNAs and the ribosomal 5S and 5.8S RNA, no physiological function could be directly demonstrated for any of them at the molecular level. The RNA of particular interest in the present study has been termed 7SL RNA (alternative nomenclatures are 7S scRNA[12] and ScL[13]) and it was first described as a component of some oncornaviruses[14]. It was later also shown to be a constitutive component of all uninfected cells[15]. 7SL RNA was usually obtained in cytoplasmic cell fractions, where it was found associated with polysomes or microsomal membranes[12,13,16], although some investigators also detected it in nuclear fractions[17]. It is a relatively abundant small RNA which has been highly conserved through evolution[12,15,17] and it was recently sequenced by two independent groups from either a cDNA clone of the human RNA[18,19] or by direct RNA sequencing of the rat RNA[20]. Both sequences are essentially identical and confirmed a previous observation[21] that long stretches of 7SL RNA are homologous to the Alu family DNA sequences. Thus, the ~300-nucleotide long 7SL RNA was shown for about 100 nucleotides at its 5′ end and ~50 nucleotides at its 3′ end[18,20] to have about 80% homology with the Alu consensus sequence[22]. The core portion of 7SL RNA (~150 nucleotides) showed no homology to Alu DNA, and is complementary to a new family of repeated DNA (but repeated at a lower frequency than Alu DNA) in the genome[18].

We demonstrate here that 7SL RNA is part of a ribonucleoprotein (RNP). This RNP is identical to the previously purified and characterized signal recognition protein[1], the name of which we consequently change to signal recognition particle (SRP). We show that the RNA is indispensable for SRP's function. Thus, 7SL RNA has a function in the process of protein translocation across the endoplasmic reticulum.

SRP contains a RNA moiety

In our studies on SRP we noticed a relatively high ratio of the absorbances at 260 to absorbance at 280 nm in our SRP prepar-

ations isolated by hydrophobic chromatography[1]. To determine whether this property was truly associated with SRP, we further purified SRP by DEAE chromatography and sucrose gradient centrifugation[1]. Analysis of the sucrose gradients revealed a higher absorbance at 254 nm (Fig. 1*B*) than at 280 nm (Fig. 1*A*) in the 11S peak fraction. The 11S peak was collected (as indicated by the horizontal bars in Fig. 1*A*, *B*) and an absorption spectrum was recorded. From the spectrum (Fig. 1*C*) it was apparent that SRP had a relative absorption maximum at 258.5 nm. This finding strongly suggested that SRP contained a nucleic acid component which co-purified with the six polypeptide chains previously identified as protein components of SRP[1] (compare the polypeptide profile of the material before and after sucrose gradient centrifugation Fig. 1*D*, lanes *a* and *b*). As most of the absorbance at 260 nm could be rendered cold acid-soluble by base hydrolysis (see Table 1), we concluded that SRP contained a RNA moiety. We will refer to this RNA as SRP-RNA.

The RNA is required for SRP function

To demonstrate the involvement of SRP-RNA in the functions of SRP, we used *in vitro* assays for the SRP-dependent translocation of secretory proteins across microsomal membranes. Two principal activities of SRP can be distinguished in these assays. First, SRP restores the ability of salt-extracted microsomes to translocate nascent secretory proteins[1,7]. If a mixture of bovine pituitary mRNA and rabbit reticulocyte mRNA was translated in the wheat germ cell-free system in the presence of salt-extracted microsomes, preprolactin and globin were synthesized (Fig. 2*A*, lane *a*). Only when the system was supplemented with purified SRP did translocation and processing of the secretory protein take place (note the disappearance of preprolactin and the appearance of prolactin in Fig. 2*A*, lane *b*).

Our second assay for SRP activity is based on the observation that SRP in the absence of microsomal membranes specifically inhibits the translation of secretory but not of cytoplasmic proteins[3]. The presence of SRP in a translation system devoid of microsomal membranes therefore caused a severe decrease in the amount of preprolactin synthesized (Fig. 2*D*, compare lanes *a* and *b*), but did not affect the amount of globin synthesized.

To test whether SRP-RNA is a constitutive and indispensable part of SRP, we treated SRP with micrococcal nuclease. As this nuclease is Ca^{2+} dependent, it can be conveniently inactivated by the addition of Ca^{2+}-chelators[23]. A rapid decrease of the translocation activity (Fig. 2*C*) and of the elongation arresting activity (Fig. 2*F*) was observed with increasing digestion time, when compared with the control values of an incubation

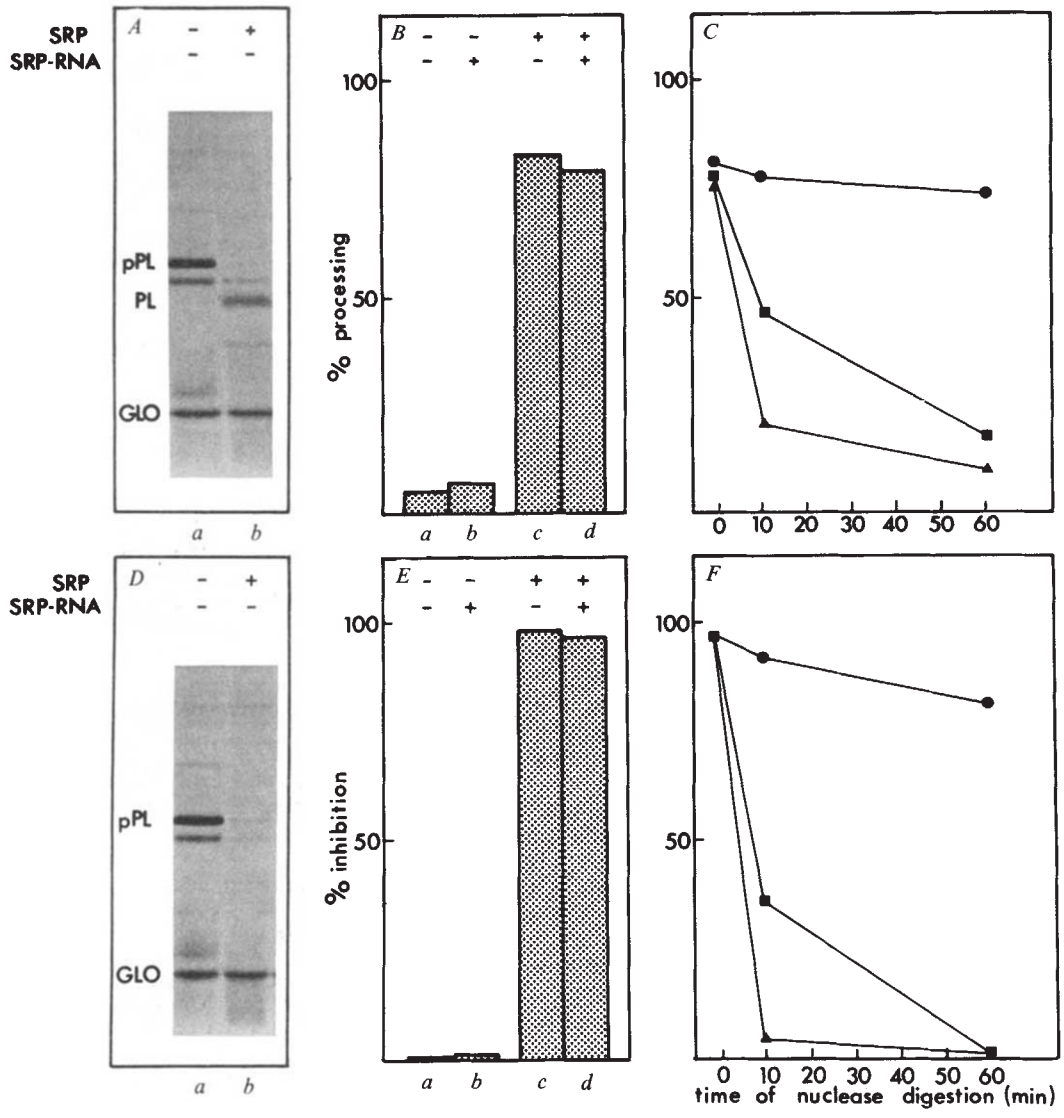

Fig. 2 SRP-RNA is required for SRP's function. Bovine pituitary and rabbit reticulocyte RNA were translated together in a wheat germ cell-free system (25 μl) either in the presence (panels *A*–*C*) or in the absence (panels *D*–*F*) of 1 equivalent of salt-extracted microsomes as described previously[3]. In panels *A*, *B*, *D* and *E* translations were supplemented with 10 U (ref. 3) of gradient-purified SRP (see Fig. 1) where indicated (SRP+). In panels *B* and *E* the translations also contained 600 ng of SRP-RNA (see Fig. 4) where indicated (SRP-RNA+). Translation products were displayed by SDS-polyacrylamide gel electrophoresis and visualized by autoradiography as shown in panels *A* and *D*. Bands corresponding to preprolactin (pPL), prolactin (PL) and globin (GLO) are indicated. The minor band between pPL and PL is pregrowth hormone. Its processed form (growth hormone) migrates as a band below PL (panel *A*, lane *b*). For quantitative interpretation, the bands corresponding to pPL and PL were excised from the gel and their radioactivity determined as described previously[34]. From the measurements obtained, per cent processing[3] (panels *B*, *C*) and per cent inhibition[8] (panels *E*, *F*) were calculated. In panels *C* and *F*, SRP was digested with *Staphylococcus aureus* nuclease (Boehringer) before it was used to supplement the translation systems. Fractions (10 μl) of gradient-purified SRP (see Fig. 1) were diluted on ice with 40 μl of a digestion mix to yield final concentrations of 1 mM $CaCl_2$ and 0 U ml^{-1} (circles), 150 U ml^{-1} (squares) or 750 U ml^{-1} (triangles) nuclease, respectively. Incubation was carried out at 30 °C. After 0, 10 and 60 min of digestion, aliquots (10 μl) were withdrawn and the nuclease was inactivated by the addition of 1 μl 20 mM EGTA. A 3-μl aliquot from each time point was assayed for SRP activity in 25 μl translations and the results quantitated as described above. Background (−SRP) and control (+SRP) values can be taken from the data in panels *B* and *E* (lanes *a* and *c*, respectively) because the data were plotted on a comparable scale.

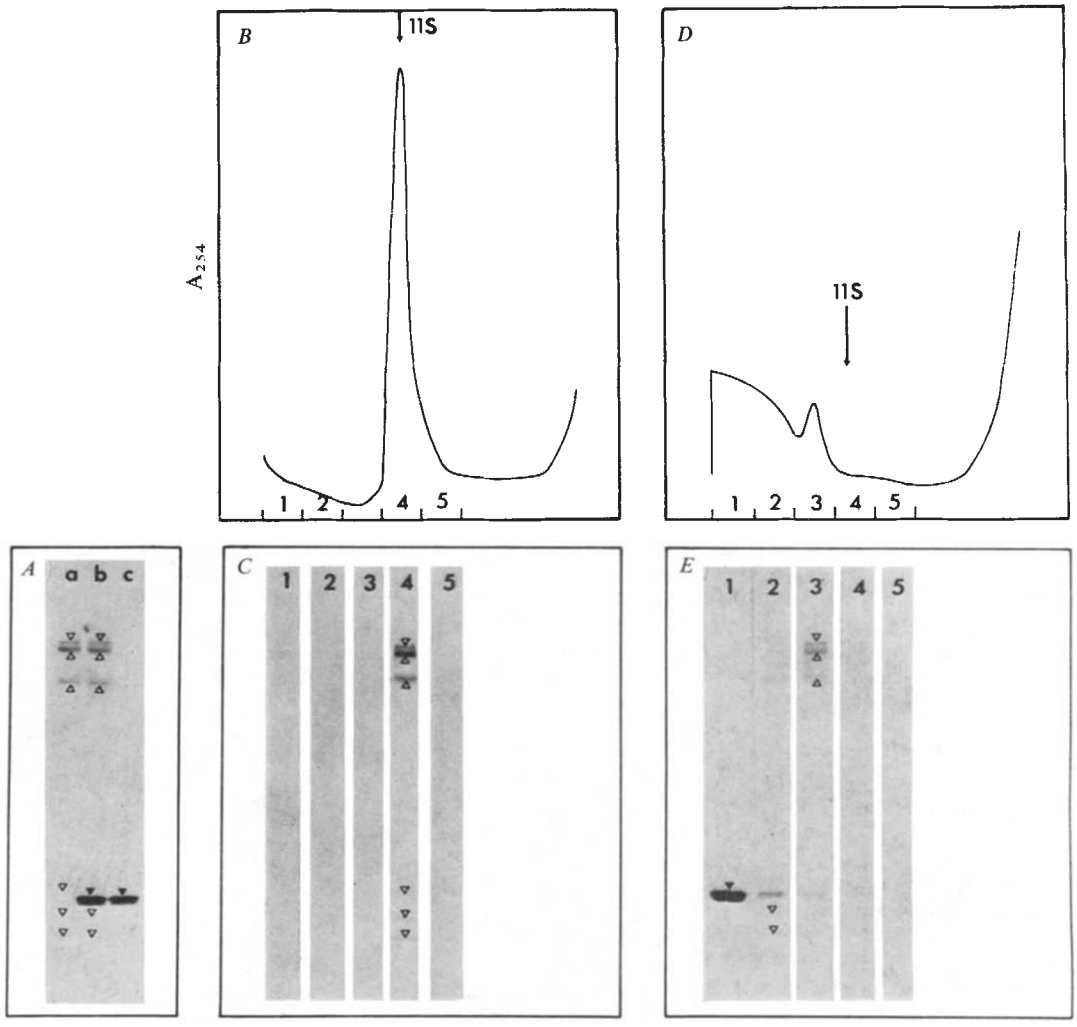

Fig. 3 SRP proteins change their sedimentation behaviour on nuclease digestion. Aliquots of gradient-purified SRP (see Fig. 1) were incubated in the absence or presence of 750 U ml^{-1} of nuclease as described in Fig. 2 legend, except that the reactions were scaled up 10-fold. After incubation, an aliquot (100 μl) of each reaction mixture (panel *A*, lane *a* (no nuclease), lane *b* (750 U ml^{-1} nuclease)) and 75 U nuclease (panel *A*, lane *c*) was TCA precipitated and the polypeptides displayed by SDS-polyacrylamide gel electrophoresis and visualized by Coomassie blue staining. Another aliquot (250 μl) of the reaction mixture was layered on top of a 5–20% sucrose gradient (5 ml) in 50 mM TEA, 500 mM KOAc, 2 mM EDTA, 0.01% Nikkol and centrifuged for 6 h at 50,000 r.p.m. in a Beckman SW50.1 rotor. Gradients were fractionated using an ISCO gradient fractionator. Absorbance was monitored at 254 nm (panel *B*, no nuclease; panel *D*, 750 U ml^{-1} nuclease), five fractions were collected as indicated, TCA precipitated and the polypeptides displayed by SDS-polyacrylamide gel electrophoresis and Coomassie blue staining (panels *C*, *E*). Bands corresponding to the six SRP proteins are marked with open arrow heads, bands contributed by the nuclease (see panel *A*, lane *c*) are marked with solid arrow heads.

where the nuclease was omitted. The effect is concentration dependent with respect to nuclease, because higher nuclease concentrations lead to a more rapid inactivation of SRP. Note, however, that to see a marked effect these digestion conditions had to be relatively harsh (for example, 150 and 750 U ml^{-1} nuclease for 10–60 min at 30 °C) compared with the nuclease treatment routinely given to microsomal membrane fractions or translation systems to deplete them of endogenous mRNA activity (20 U ml^{-1} nuclease for 5 min at 25 °C). It is therefore not surprising that no loss of translocation activity of microsomal membranes was detected previously on mild nuclease treatment[2,24].

Analysis of the polypeptide profile of SRP before and after nuclease treatment (Fig. 3*A*, lanes *a*, *b*) revealed that the electrophoretic mobility of five of the six polypeptides was not altered (the sixth was buried under a band contributed by the nuclease and could therefore not be analysed). Taken together with the fact that SRP incubated with nuclease but in the presence of both Ca^{2+} and EGTA was not inactivated (data not shown), the explanation that the loss of SRP activity on nuclease digestion was due to a protease contamination can be ruled out.

RNase treatment changes the sedimentation behaviour of the SRP proteins

When nuclease-treated SRP was analysed by sucrose gradient centrifugation, the sedimentation characteristics of the SRP proteins appeared changed. Whereas SRP incubated in the absence of nuclease sedimented at 11S (Fig. 3*B*, *C*) as previously described (ref. 1 and Fig. 1), on extensive nuclease digestion the sedimentation of the SRP proteins was retarded, although they still did not sediment as monomeric species (Fig. 3*D*, *E*). Interestingly, two subfractions seemed to be resolved, one containing the three high molecular weight proteins sedimenting at about 8S and one containing two (possibly all

Table 1 Stoichiometry between protein and RNA components in SRP

	RNA (μg per 100 μg SRP)	Protein
Assay	21	79
Calculated	27	73

For the assay, gradient-purified SRP was treated with 0.3 M KOH for 1 h at 60 °C. After precipitation with cold $HClO_4$ the RNA content of SRP was calculated from the absorbance at 260 nm of the supernatant fraction[32]. Absorbance measurements were converted into μg RNA by assuming an average nucleotide molecular weight of 330 and an average nucleotide molar extinction coefficient of 10^4 at 260 nm. Protein in the SRP fraction was determined according to Schaffner and Weissman[33] using bovine serum albumin as a standard. According to these measurements our SRP preparation (20 U μl^{-1} (ref. 1), see Fig. 1) contained 75 μg ml^{-1} RNA and 285 μg ml^{-1} protein. The proportions were calculated based on our size estimations of SRP-RNA (260 nucleotides) and the molecular weights of the six SRP proteins as estimated by SDS-polyacrylamide gel electrophoresis (see ref. 1 and Fig. 1). SRP was assumed to consist of one molecule of each of these components.

three, see above) of the low molecular weight proteins sedimenting at about 5S.

Isolated SRP-RNA has no measurable activity

It was previously reported that the isolated RNA of a cytoplasmic RNP fraction possessed the same translation inhibitory activity as the intact particles[25]. To test whether isolated SRP-RNA would exhibit a direct effect in our assay systems, SRP-RNA was extracted from a gradient-purified SRP preparation. It was then determined whether it would exhibit either a SRP-like activity by itself or whether it could be shown to compete with intact SRP. As shown by the data in Fig. 2*B* and *E*, the isolated SRP-RNA (even in eightfold higher molar concentrations than a saturating amount of SRP) neither restored translocation competence to salt-extracted microsomes (Fig. 2*B*, compare lanes *a* and *b*) nor inhibited translation of prolactin mRNA (Fig. 2*E*, compare lanes *a* and *b*) or globin mRNA (data not shown). When SRP was assayed in the presence of an eightfold molar excess of SRP-RNA, the SRP-RNA also did not compete with SRP in either of the assays (Fig. 2*B*, *E*, lanes *c*, *d*).

Characterization of the SRP-RNA

From the above experiments we conclude that the RNA moiety is a constitutive part of SRP in a structural as well as functional sense. We therefore attempted to characterize this SRP-RNA more carefully. When the extracted RNA was electrophoresed on a polyacrylamide gel in denaturing conditions, one major and one minor band could be resolved on ethidium bromide staining (Fig. 4*A*). From the staining intensity we estimated that the major band (slower mobility) was comprised of about four times more RNA than the lower molecular weight band.

Having established that SRP-RNA appeared to be of a discrete size(s), we attempted to label the molecules at the 3′ end using T_4 RNA ligase and 5′-^{32}P-pCp. The pattern of the 3′-labelled SRP-RNA obtained after autoradiography of a polyacrylamide gel (Fig. 4*B*) was identical (qualitatively as well as quantitatively) to that obtained after ethidium bromide staining (compare with Fig. 4*A*). We also labelled a small nuclear RNA (snRNA) fraction from HeLa cells (a gift of Dr D. Adams) with 5′-^{32}P-pCp and used it as markers in this electrophoresis system (Fig. 4*C*). From the sizes of the snRNAs[11], we extrapolated the size of the SRP-RNA to be about 260 nucleotides and 245 nucleotides for the major and the minor molecular weight species, respectively (Fig. 4*D*).

Relationship of SRP-RNA to 7SL RNA

To determine the possible relationship of SRP-RNA to any known RNA sequences, we performed partial sequence analysis. The 260-nucleotide and 245-nucleotide bands of 3′-labelled

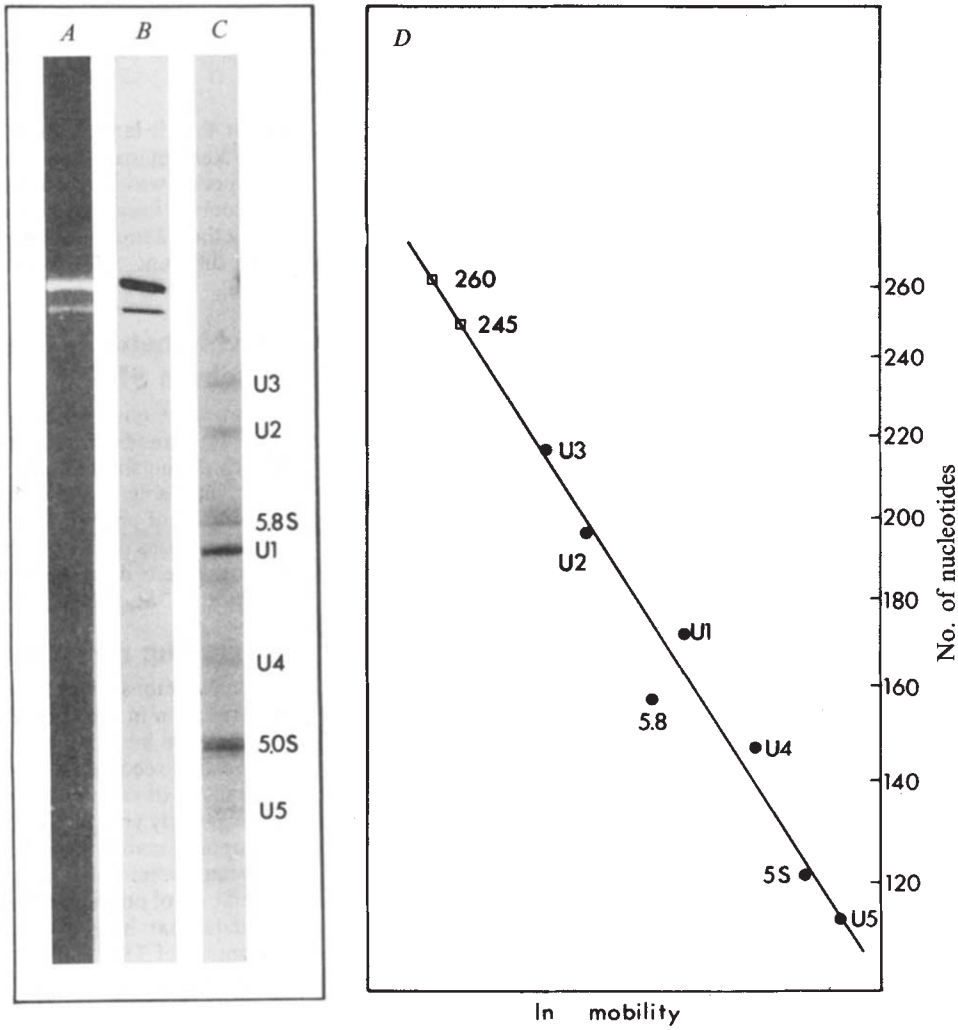

Fig. 4 Size characterization of SRP-RNA. RNA was extracted by the EtOH/perchlorate procedure[35] after proteinase K treatment of gradient purified SRP. First we concentrated SRP further by EtOH precipitation. To an 800-μl fraction of gradient-purified SRP we added 2 ml of EtOH. The mixture was kept for 30 min at −80 °C and SRP was pelleted by centrifugation for 15 min at 10,000 g_{av}. The wet pellet was dissolved in 120 μl of a solution containing 25 mM TEA, 2.4% SDS, 100 mM NaCl, 15 mM EDTA and 200 μg ml^{-1} proteinase K (Boehringer). The mixture was incubated at 37 °C for 30 min, then 80 μl of a solution of 3.5 M $NaClO_4$ was added and the mixture heated to 50 °C for 5 min. A saturated solution (800 μl) of $NaClO_4$ in EtOH/water (80:20) was added, the mixture was incubated for 45 min on ice and the RNA was pelleted for 15 min at 10,000 g_{av}. The pellet was taken up in 50-μl sterile 300 mM NaOAc, 1 mM EDTA and reprecipitated with 125 μl of EtOH after a 30-min incubation at −80 °C. This step was performed twice more. The final pellet was rinsed with 100 μl ice-cold EtOH/water (80:20), lyophilized to dryness and taken up in sterile water. The yield was 60 μg of RNA based on absorbance at 260 nm (20 A_{260} units ≡ 1 mg). SRP-RNA was labelled at the 3′ end following the procedure of England *et al.*[36]. A sample of 0.4 μg RNA was incubated with 25 pmol 5′-^{32}P-pCp (NEN) and 500 U ml^{-1} T_4-RNA ligase (PL Biochemicals) for 8 h at 4 °C. Carrier tRNA (6 μg, Boehringer, calf liver) was added and the RNA reisolated by EtOH/perchlorate precipitation, followed by EtOH precipitation and a final rinse with 80% EtOH. 2% Of the label was incorporated into SRP-RNA. A sample of 0.4 μg snRNA from HeLa cells was labelled by the same procedure. The isolated SRP-RNA (2 μg, lane *A*), the 3′-labelled SRP-RNA (1,000 d.p.m., lane *B*) and the 3′-labelled HeLa snRNA (10,000 d.p.m.) were denatured in 50% formamide in 50 mM Tris, 50 mM boric acid, 2 mM EDTA (TBE) for 4 min at 50 °C and electrophoresed in a 50-cm long, 0.4-mm thick 10% polyacrylamide gel containing 50 mM TBE and 7 M urea at 1,000 V until the xylene cyanole marker dye was 10 cm from the bottom. The gel was stained in 1 μg ml^{-1} ethidium bromide for 30 min, destained for 30 min in water, photographed wet under UV light (lane *A*) and dried. Radioactive bands were visualized by autoradiography (lanes *B*, *C*). The HeLa snRNAs were assigned according to ref. 37 and their sizes[11] were taken to be: U3, 216 nucleotides (NT); U2, 196 NT; U1, 171 NT; 5.8S, 158 NT; U4, 147 NT; 5.0S, 121 NT; U5, 114 NT. The standard curve (panel *D*) was constructed by plotting the square root of the number of nucleotides over the logarithm of the relative mobility[38] and fitting a straight line by the least-square method.

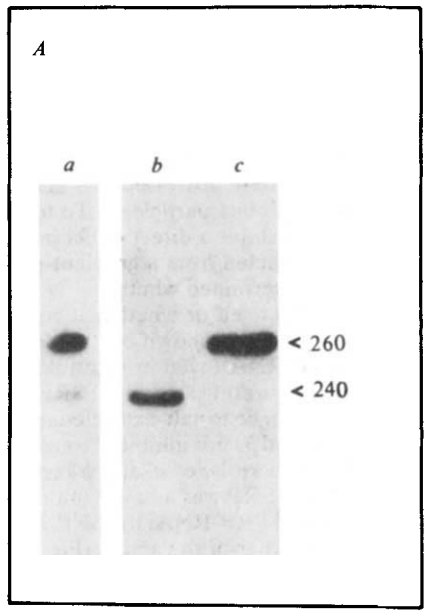

Fig. 5 (Right and opposite page.) Partial sequence determination of SRP-RNA. The 260- and the 245-nucleotide long 3'-labelled SRP-RNAs were separated by polyacrylamide gel electrophoresis[28] as described in Fig. 4 legend except that the gel was 7%, 30 cm long and 1.2 mm thick (panel *A*, lane *a*). Bands were localized by autoradiography of the wet gel, excised with a sterile scalpel, each rinsed for 30 min with 1 ml of sterile water and eluted on an overhead shaker overnight at 37 °C into 1 ml of sterile 0.5 M NH_4OAc, 1 mM EDTA, 10 μg ml^{-1} tRNA. The eluate was filtered through a 0.22-μm Millipore filter, EtOH precipitated and reprecipitated from 100 μl 300 mM NaOAc, 1 mM EDTA with 250 μl EtOH. The pellet was rinsed with 100 μl 80% EtOH and lyophilized. Aliquots were re-electrophoresed in the conditions described above and showed no breakdown or cross-contamination of the two species (panel *A*, lanes *b*, *c*). Chemical modification reactions followed by aniline strand cleavage were performed as described by Peattie[26] with the following modifications: the 'A reaction' contained 2 μl diethylpyrocarbonate and 10 μl EtOH; incubation was for 10 min. The 'G, C and U reactions' were incubated for 1, 20 and 12 min, respectively. The cleaved RNA was denatured in 50% formamide, 50 mM TBE and electrophoresed on a 40-cm long, 0.4-mm thick 20% polyacrylamide gel in 100 mM TBE (acrylamide to bisacrylamide in all sequencing gels was 20:1) in a 37 °C incubator at 1,000 V until the bromphenol blue marker dye was 20 cm from the bottom. The autoradiogram of the wet gel is shown in panel *B*. 10,000 d.p.m. were loaded per lane. Cleavage products of the 260-nucleotide SRP-RNA of the C, U, G and A-reaction are shown in lanes 1, 2, 3 and 4, respectively. Cleavage products of the 245-nucleotide SRP-RNA of the A reaction are shown in lane 5. The sequence assignments are indicated by dots on the bands. The numbering of the assigned residues is according to Ullu *et al.*[18] (see also Fig. 6). The position of the marker dyes bromphenol blue (BPB) and xylene cyanole (XC) is indicated. On parallel lanes (not shown) cleavage products of 3'-labelled 5S RNA of *Bombyx mori* were electrophoresed to confirm the fidelity of the sequencing reactions on the basis of its known sequence[39]. The arrow at the bottom indicates the position of the 3'-terminal U residue of this 5S RNA. Its larger fragments migrated in the same positions as the SRP-RNA cleavage products. Residue 284 of SRP-RNA could not be unambiguously assigned. We used enzymatic sequencing reactions to determine a partial sequence further into the molecule. The reactions using U_2 RNase (cleaves after A residues) and T_1 RNase (cleaves after G residues) were carried out according to Donis-Keller *et al.*[27] in 7 M urea at 50 °C, except that the reaction volumes were scaled down to 10 μl and the carrier tRNA was at 100 μg ml^{-1}. We also performed a partial base hydrolysis[27] (cleaves the RNA randomly) and a control incubation in the presence of urea at elevated temperature without the addition of nuclease. Cleavage products were displayed by electrophoresis in an 8% polyacrylamide gel as described above and visualized by autoradiography of the dried gel. Electrophoresis was terminated after the xylene cyanole marker dye had moved 25 cm (panel *C*) and 50 cm (panel *D*) through the gel. Panel *C*: Lane 1, chemical A cleavage; lane 2, enzymatic cleavage with U_2 at 10 U ml^{-1}; lane 3, enzymatic cleavage with U_2 at 3 U ml^{-1}; lane 4, base ladder; lane 5, enzymatic cleavage with T_1 at 0.01 U ml^{-1}; lane 6, enzymatic cleavage with T_1 at 0.003 U ml^{-1}; lane 7, control (incubation in the absence of nuclease). Panel *D*: Lane 1, enzymatic cleavage with U_2 at 10 U ml^{-1}; lane 2, base ladder; lane 3, enzymatic cleavage with T_1 at 0.003 U ml^{-1}; lane 4, control (incubation in the absence of nuclease). The assignment of A and G residues is indicated by dots; Y indicates pyrimidine residues (C or U, which cannot be distinguished by this method), N indicates residues which could not be assigned because of ambiguous cleavage reactions or major fragments in the control lane. In panel *D* the base ladder bands were compressed and no sequence could be read between residues 188 and 191.

SRP-RNA were separated by preparative polyacrylamide electrophoresis and eluted from the gel (Fig. 5*A*, lane *a*). On re-electrophoresis they migrate as distinct bands of unchanged mobility (Fig. 5*A*, lanes *b*, *c*) and therefore appear not to be interconvertible conformational isomers of each other. We then subjected the 260-nucleotide SRP-RNA species to sequence analysis by either a complete set of chemical[26] (Fig. 5*B*) or a partial set of enzymatic[27] (Fig. 5*C*) cleavage reactions followed by polyacryamide gel electrophoresis of the generated fragments[28] and autoradiography. The cleavage pattern allowed us to read the complete sequence of the SRP-RNA for 40 residues from the 3' end (Fig. 5*B*) and a partial sequence (only the A and G residues) for about 150 residues from the 3' end (Fig. 5*C*).

When we compared our partial sequence data (Fig. 6, line *c*) with the recently published sequences for 7SL RNA from man[18] and rat[20] (Fig. 6, lines *a*, *b*), we found a perfect match in the sequence alignments (Fig. 6). Furthermore, our partial sequence is distinct from 7SK RNA (ref. 19 and E. Ullu, personal communication), the only other major small cytoplasmic RNA in the size class of interest. Both HeLa cell 7SL RNA and the 260-nucleotide SRP-RNA have an identical electrophoretic mobility in polyacrylamide gels (E. Ullu, personal communication) and we therefore attribute the apparent size difference between our estimation (260 nucleotides) and the published sizes for 7SL RNA [303 (ref. 18) and 295 (ref. 20) nucleotides] to either an anomalous behaviour of the RNA on electrophoresis or an inadequacy in our size extrapolation. We conclude that SRP-RNA is identical to 7SL RNA, although minor differences at the 5' end between the published forms of 7SL RNA and SRP-RNA cannot be ruled out.

We also subjected the 245-nucleotide long SRP-RNA species to a partial chemical sequencing reaction (allowing us to read the A residues). For the last 40 residues on the 3' end we obtained an identical cleavage pattern for the 260-nucleotide (Fig. 5*B*, lane 4) and the 245-nucleotide (Fig. 5*B*, lane 5) SRP-RNA, indicating that both bands have an identical 3'-terminal sequence. This identity in the cleavage pattern could be followed from the 3' end through the entire molecule if the fragments were displayed on lower percentage polyacrylamide gels (data not shown). We therefore conclude that the 245-nucleotide species was identical to the 260-nucleotide species except that it lacked about 15 nucleotides at its 5' end. The most likely interpretation for this finding is that the 245-nucleotide species was derived from the 260-nucleotide molecule as a nucleolytic breakdown product. This interpretation is supported by the finding that the ratio of the two bands was variable when different SRP preparations were analysed (data not shown).

Stoichiometry between RNA and protein in SRP

We have previously estimated from the Coomassie blue staining intensity of the SRP proteins that SRP contains one molecule of each of the six different polypeptide chains[1]. The data displayed in Table 1 show that the experimentally determined proportions of protein to RNA correspond reasonably well to the proportions calculated from our molecular weight determinations. These data therefore suggest that there is also one molecule of 7SL RNA per six polypeptide chains in SRP.

Concluding remarks

We have demonstrated here that 7SL small cytoplasmic RNA has a function in the early step of protein secretion and membrane protein insertion as a constitutive and indispensable part of the signal recognition particle. SRP was previously isolated by means of its distinct interaction with hydrophobic matrixes[1] as a negatively charged, stable particle containing six proteins. Its proposed complex mode of transient interactions[9] with the membrane-bound SRP receptor[9-11], with ribosomes[3], and with a specific set of polysomes[3] might explain some of the contradictory data that had accumulated concerning the subcellular localization of 7SL RNA[13,14,16-18]. Although we do not know whether all 7SL RNA is found in the cell as SRP, the availability of specific antibodies against three of the SRP proteins (P.W. and G.B., in preparation) should allow us to answer this question conclusively.

It is not clear what function 7SL RNA serves in SRP, but two different modes of action could be envisaged: (1) the RNA could have a merely structural role and could serve as a 'core' or 'matrix' on which the SRP proteins (or perhaps other accessory proteins like the SRP receptor or ribosomal proteins

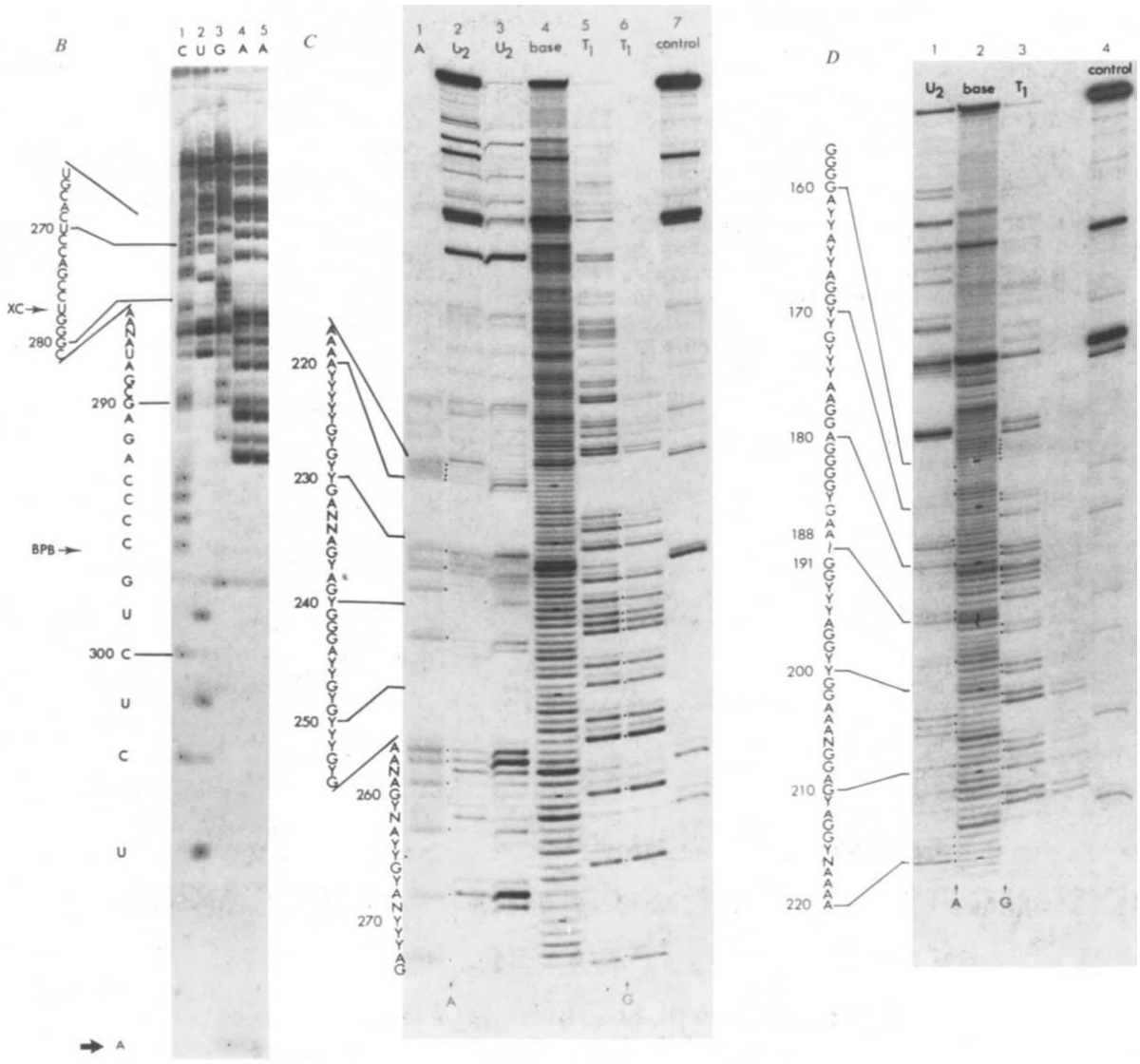

transiently) assemble and/or (2) the RNA could be involved in specific base-pairing interactions with other nucleic acid molecules (likely candidates would be rRNA or specific mRNAs or tRNAs) in the course of SRP action. A direct interaction of SRP with ribosomes was observed and this interaction was strengthened when mRNAs coding for secretory proteins were translated[3]. Both interactions could, however, be abolished when SRP proteins were modified by alkylation with *N*-ethylmaleimide[3]. Although these data support the importance of protein–protein interactions, the additional involvement of specific RNA–RNA interactions is still an attractive possibility. Base pairing could provide weak, but highly specific interactions (like the codon–anticodon interaction), requiring reinforcement by specific proteins to be productive.

7SL RNA consists of a 140-nucleotide stretch of a new family of repeated sequences which is flanked on both ends by regions homologous to the highly repeated Alu family[18,20,21]. Our sequence analysis went from the 3′ end across the region homologous to the Alu DNA well into the centre part. We therefore feel certain that SRP-RNA is identical to the sequenced 7SL RNA. The function of the Alu sequences in the 7SL RNA or in SRP is not known. Whether they have a role primarily in the transcription of the RNA (7SL RNA is a polymerase III transcript[29] and Alu sequences function as fairly strong promotors for this polymerase[30]) or whether they play an integral part in the structure and function of SRP remains to be established. As Alu-like sequences seem to be packaged into a compact, specific and evolutionarily highly conserved

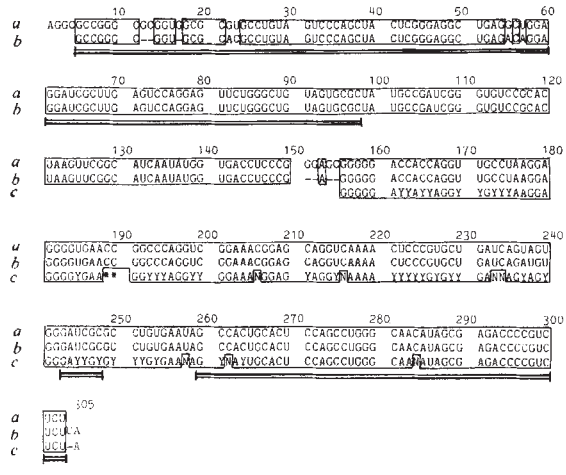

Fig. 6 Sequence comparison of 7SL RNA with SRP-RNA. The sequences of Ullu *et al.*[18] (*a*) and Yi *et al.*[20] (*b*) of 7SL RNA were aligned and compared with our partial sequence of SRP-RNA (*c*). Matching nucleotides are boxed. We excluded from the box all sequence positions where no assignment was made (N) and the unassigned band compression region (*). No mismatch between both 7SL RNAs and the SRP-RNA sequence was detected. Regions in 7SL RNA that were shown to be homologous to Alu DNA sequences are indicated with bars. The numbering of the residues is according to Ullu *et al.*[18].

(see below) RNP structure (SRP), the provocative possibility arises that Alu-like sequences could have arison by re-iteration from SRP-RNA (rather than the unique core of SRP-RNA having picked up Alu-like sequences from the genome).

Both the 7SL RNA and the mode of co-translational protein translocation seem to be highly conserved through evolution[31]. We have recently demonstrated that the prokaryotic secretory protein β-lactamase, when translated on plant ribosomes (wheat germ), is translocated and correctly processed by mammalian microsomal membranes[5]. This translocation process was SRP dependent and the synthesis of the prokaryotic secretory protein could be arrested by SRP in the absence of microsomal membranes. These findings strongly suggest that the mechanism of co-translational protein translocation has been conserved and encourage our search for a prokaryotic counterpart of SRP and its small RNA. Thus, SRP seems to be an integral and indispensable component of the protein synthesis machinery, ensuring the correct topogenesis of a specific subset of proteins. Considering its structural features and its intimate (although probably transient) functional association with ribosomes, it could almost be regarded as a 'third ribosomal subunit' functioning as the adapter between the cytoplasmic translation and the membrane-bound protein translocation machinery.

We thank D. Adams and M. Walberg for their advice and help concerning the RNA sequencing technology, P. Lizardi, H. Robertson, J. Steitz and A. Weiner for many helpful discussions and suggestions, and E. Ullu for making the sequence of 7SL RNA available to us prior to its publication. These studies were supported by NIH research grant GM-27155. P.W. is supported by a research fellowship from the Deutsche Forschungsgemeinschaft (Wa 478/1-1). Original prints of Fig. 5 are available on request from the authors.

Received 22 June; accepted 3 August 1982.

1. Walter, P. & Blobel, G. *Proc. natn. Acad. Sci. U.S.A.* **77,** 7112–7116 (1980).
2. Warren, G. & Dobberstein, B. *Nature* **273,** 569–571 (1978).
3. Walter, P., Ibrahimi, I. & Blobel, G. *J. Cell Biol.* **91,** 545–550 (1981).
4. Stoffel, W., Blobel, G. & Walter, P. *Eur. J. Biochem.* **120,** 519–522 (1981).
5. Mueller, M., Ibrahimi, I., Chang, C. N., Walter, P. & Blobel, G. *J. biol. Chem.* (in the press).
6. Anderson, D. J., Walter, P. & Blobel, G. *J. Cell Biol.* **93,** 501–506 (1982).
7. Walter, P. & Blobel, G. *J. Cell Biol.* **91,** 551–556 (1981).
8. Walter, P. & Blobel, G. *J. Cell Biol.* **91,** 557–561 (1981).
9. Gilmore, R., Walter, P. & Blobel, G. *J. Cell Biol.* (in the press).
10. Meyer, D. I., Krause, E. & Dobberstein, B. *Nature* **297,** 647–650 (1982).
11. Busch, H., Reddy, R., Rothblum, L. & Choi, Y. C. *A. Rev. Biochem.* **51,** 617–653 (1982).
12. Walker, T. A., Pace, N. R., Erikson, R. L., Erikson, E. & Behr, F. *Proc. natn. Acad. Sci. U.S.A.* **71,** 3390–3394 (1974).
13. Zieve, G. & Penman, S. *Cell* **8,** 19–31 (1976).
14. Bishop, J. M. *et al. Virology* **42,** 927–937 (1970).
15. Erikson, E., Erikson, R. L., Henry, B. & Pace, N. R. *Virology* **53,** 40–46 (1973).
16. Gunning, P. W., Beguin, P., Shooter, E. M., Austin, L. & Jeffrey, L. *J. biol. Chem.* **256,** 6670–6675 (1981).
17. Reddy, R. *et al. J. biol. Chem.* **256,** 8452–8457 (1981).
18. Ullu, E., Murphy, S. & Melli, M. *Cell* **29,** 195–201 (1982).
19. Ullu, E. & Melli, M. *Nucleic Acids Res.* **10,** 2209–2223 (1982).
20. Li, W. Y., Reddy, R., Henning, D., Epstein, P. & Busch, H. *J. biol. Chem.* **257,** 5136–5142 (1982).
21. Weiner, A. *Cell* **22,** 209–218 (1980).
22. Deininger, P. L., Jolly, D. J., Rubin, C. M., Friedmann, T. & Schmid *J. molec. Biol.* **151,** 17–33 (1981).
23. Pelham, H. R. B. & Jackson, R. J. *Eur. J. Biochem.* **67,** 247–256 (1976).
24. Walter, P. & Blobel, G. *Meth. Enzym.* (in the press).
25. Mukherjee, A. K. & Sarkar, S. *J. biol. Chem.* **256,** 11301–11306 (1981).
26. Peattie, D. A. *Proc. natn. Acad. Sci. U.S.A.* **76,** 1760–1764 (1979).
27. Donis-Keller, H., Maxam, A. M. & Gilbert, W. *Nucleic Acids Res.* **4,** 2527–2538 (1977).
28. Maniatis, T. & Efstratiadis, A. *Meth. Enzym.* **65,** 299–305 (1980).
29. Zieve, G., Benecke, B. & Penman, S. *Biochemistry* **16,** 4520–4525 (1977).
30. Duncan, C. *et al. Proc. natn. Acad. Sci. U.S.A.* **76,** 5095–5099 (1979).
31. Talmadge, K., Stahl, S. & Gilbert, W. *Proc. natn. Acad. Sci. U.S.A.* **77,** 3369–3373 (1980).
32. Fleck, A. & Munro, H. N. *Biochim. biophys. Acta* **55,** 571–583 (1962).
33. Schaffner, W. & Weissman, C. *Analyt. Biochem.* **56,** 502–504 (1973).
34. Walter, P., Jackson, R. C., Marcus, M. M., Lingappa, V. R. & Blobel, G. *Proc. natn. Acad. Sci. U.S.A.* **76,** 1795–1799 (1979).
35. Lizardi, P. M. & Engelberg, A. *Analyt. Biochem.* **98,** 116–122 (1979).
36. England, T. E., Bruce, A. G. & Uhlenbeck, O. C. *Meth. Enzym.* **65,** 65–74 (1980).
37. Lerner, M. R., Boyle, J. A., Mount, S. M., Wolin, S. L. & Steitz, J. A. *Nature* **283,** 220–224 (1980).
38. Lehrach, H., Diamond, D., Wozney, J. M. & Boedtke, H. *Biochemistry* **16,** 4743–4751 (1977).
39. Komiya, H., Kawakami, M. & Takemura, S. *J. Biochem.* **89,** 717–722 (1981).

Mitochondrial and chloroplast genomes of maize have a 12-kilobase DNA sequence in common

David B. Stern* & David M. Lonsdale

Plant Breeding Institute, Maris Lane, Trumpington, Cambridge CB2 2LQ, UK

A 12-kilobase DNA sequence has been identified in the maize mitochondrial genome which is homologous to part of the inverted repeat of the maize chloroplast genome. In chloroplasts the sequence contains a 16S rRNA gene, and also the coding sequences for tRNA^{Ile} and tRNA^{Val}. Mitochondrial DNA from the male-sterile cytoplasms of maize is altered in this region.

INTERACTIONS between the nucleus and cytoplasmic organelles have a major role in eukaryotic cellular metabolism. Mitochondrial and chloroplast ATPases and some cytochromes, for example the yeast cytochrome *c* oxidase complex, are assembled post-translationally in the organelles from both nuclear and organelle encoded polypeptide subunits[1–9].

Although eukaryotic cells depend on the interactions of organellar gene products, the genetic material of the nucleus, mitochondrion and chloroplast is usually thought of as being maintained discretely in each organelle without duplication elsewhere. We report here, however, the characterization of a 12-kilobase (kb) DNA sequence that is found in both the chloroplast and mitochondrial genomes of maize. The similarity of the sequences, with more than 90% base sequence homology, is striking. Furthermore, this particular region of the mitochondrial genome is altered in three male-sterile lines of maize, suggesting that the maintenance of homology may be essential to normal plant development.

* Present address: Department of Biological Sciences, Stanford University, Stanford, California 94305, USA.

Cross-hybridization between mitochondrial and chloroplast DNAs

^{32}P-labelled preparations of maize mitochondrial RNA (mtRNA) were found to hybridize weakly to two mtDNA *Sst*II restriction fragments of 1.75 and 1.58 kb (Fig. 1*a*), which were known not to contain the mitochondrial ribosomal RNA (rRNA) genes. Cosmid clones of mtDNA containing these restriction fragments, for example 83H4 (see Fig. 3*e*), hybridized weakly to the mitochondrial 18S rRNA, but much more strongly to an RNA molecule of ~1,500 nucleotides (Fig. 1*b*). As this is the size of the chloroplast 16S rRNA, the presence of which is demonstrated when total RNA is probed with a cloned wheat chloroplast 16S rDNA sequence[10], it seemed likely that the mtRNA preparations used to probe the *Sst*II mtDNA digests were contaminated with chloroplast RNA, and that some sequence homology existed between the 1.58- and 1.75-kb mitochondrial *Sst*II fragments and the chloroplast 16S rRNA.

Restriction endonuclease digests of mtDNA were therefore probed with nick-translated maize chloroplast DNA (ctDNA)

0028–0836/82/420698—05$01.00